

The Postnatal Development of the Mouse Pericardium; the Time and Mechanism of Formation of Pericardial Pores

By

Takeshi MATSUDA, Yoshifumi FUKUO, *Harumichi SHINOHARA,
Satoshi MORISAWA and Toshio NAKATANI

Department of Anatomy I, Faculty of Medicine
Toyama Medical and Pharmaceutical University, Sugitani 2630, Toyama 930-01, Japan
*Person for correspondence

—Received for Publication, November 30, 1989—

Key words: Mouse, Pericardium, Pores, Development

Summary: The mouse pericardium is a continuous serous membrane, up to postnatal day 6 (P6), that consists of pericardial and pleural mesothelia with sparse connective tissue sandwiched in between. This study shows that on P7 the pericardium becomes fenestrated, and the pericardial and pleural cavities become continuous. We found that the number of pores per pericardium increased continuously with the advance of age and reached as many as 3000 on P21.

Transmission electron microscopy of the pericardium revealed various structures of the pericardial and pleural mesothelia that may relate to the formation of the pericardial pores. The pericardial and pleural mesothelia were adjoined with cytoplasmic processes that extended toward the base of the opposing mesothelium. As a result of the adjoinment, a pair of U-shaped folds were formed. The two U-shaped folds were connected with tight junctions at their apices, and separation of these junctions may give rise to the pericardial pores.

The presence of numerous fenestrations, or pores, has been reported in the omentum (Carr, 1967) and the retrocardiac mediastinal pleura of mice (Mixer, 1941). These pores allow free passage of lymphocytes, macrophages, and other free cells, and are postulated to work with the host's immune system (Mironov *et al.*, 1979). Recently, we found similar pores in the pericardium of rodents (Nakatani *et al.*, 1988). Tracers injected into the pleural cavity flowed rapidly into the adjacent pericardial cavity through the pericardial pores. Macrophages and other free cells stimulated by the tracer also migrated through the pericardial pores. This suggests that the pores may contribute to an allied defense mechanism between the pleural and pericardial cavities of rodents (Fukuo *et al.*, 1988).

In a previous study, we noticed that the pericardial pores were not present in newborn mice. This study starts to clarify the time and mechanism of formation of these pores.

Materials and Methods

Animals

Ddy strain mice were used. They were maintained in an air-conditioned room at 21°C with light from 0700 to 1900 h and dark from 1900 to 0700 h (LD 12:12).

Water and laboratory chows were given ad libitum. One male and one female mouse were caged together overnight, and we checked for a vaginal plug the following morning. The day when the plug was found was designated as day of pregnancy. The day of delivery varied from 18 to 21 days of gestation (Snell, 1961), and was designated postnatal day 1 (P1). We used only the animals born on day 19 of gestation.

Light Microscopy (LM)

Mice were anesthetized with ether, and their anterior chest walls were opened widely. A sufficient amount of 20% formalin was dropped into the pleural cavity, and the tissue was placed in fresh fixatives for 24 hours. The parietal pericardium which completely enclosed the heart was carefully cut along the phrenic nerve to divide it into ventral and dorsal halves. Each half was further cut into two or three fragments under a dissecting microscope. The fragments were stained with 0.1% toluidine blue for 1 min, rinsed in tap water, spread and mounted on a glass slide, and examined with a light microscope ($\times 400$) to count the number of pericardial pores. After counting the pores the width of the pericardium was estimated on plotting paper ruled into 1 mm squares. Slides were prepared from 3 mice each day from days P1 to P7 and every other day from days P9

to P21. Thus forty two mice were examined throughout the experiment. The entire pericardium of each animal was sampled, and almost the entire width of the pericardium was observed.

Scanning and Transmission Electron Microscopy (SEM and TEM)

We used 12 mice at ages P1 to P21. They were prepared as described above except that cold 2% glutaraldehyde in 0.1M phosphate buffer solution (PBS) at pH 7.4 containing 5% sucrose was poured into the chest cavity. The pericardium was carefully removed under a dissecting microscope, immersed in fresh fixative for 2 h and cut into fragments during fixation. Part of the thymus, great vessels, or fatty tissue was left attached to these specimens to distinguish between the pericardial and pleural surfaces. The tissue was rinsed in PBS overnight, then postfixed in 2% osmium tetroxide in veronal acetate buffer for two hours. Some of the fragments were dehydrated in a graded ethanol series, critical-point dried, and examined with a scanning electron microscope. Other fragments were stained *en bloc* in a 0.5% aqueous solution of uranyl acetate for 2 hours. After dehydration in an ethanol series these tissues were embedded in Quetol 812. They were then ultrathin-sectioned, stained with uranyl acetate and lead citrate, and examined with a transmission electron microscope.

Results

Stage of Appearance and Counting of Pericardial Pores

Pores were not found in the pericardium from P1 to P6, but were found in all of three pericardia on P7. The mean number of pores on P7 was approximately 2 per pericardium (Fig. 1 and Table 1). These pores were clearly defined, oval in shape and 5–20 μm in diameter. The pores were distinctly visible against the light-blue background of the pericardium stained with toluidine blue. All pericardia on P7 or later had pores. A lacy appearance of the pericardium, due to the presence of numerous pores in a limited area, was found on P17 or later (Fig. 2). The pores observed under LM and SEM were usually 10 to 30 μm in diameter. A rare few were larger than 50 μm or smaller than 2 μm in diameter.

The number of pericardial pores from P1 through P21 is shown in Table 1. The area of the pericardium increased significantly with the advance of age ($r=0.91$, $p<0.01$), as did the number of pores per pericardium ($r=0.80$, $p<0.01$). Similarly, the number of pores per unit-area increased significantly with age ($r=0.81$, $p<0.01$). This means that the number of pores per pericardium increased as the area of the pericardium increased until P21. In addition, this increase was

Table 1. The number of pericardial pores

Days of life	Width (mm ²) of the pericardium examined	Number of pores		
		per pericardium		per unit area (1mm ²)
1	15.3 ± 1.5	0		0
2	15.7 ± 2.1	0		0
3	17.0 ± 1.7	0		0
4	17.0 ± 2.0	0		0
5	20.0 ± 4.9	0		0
6	19.3 ± 0.6	0		0
7	23.0 ± 4.6	2 ±	2.3	0.1 ± 0.08
9	23.0 ± 5.3*	11 ±	5.0*	0.5 ± 0.14*
11	33.7 ± 2.1	20 ±	20.3	0.6 ± 0.62
13	35.7 ± 1.2	38 ±	51.9	1.1 ± 1.44
15	30.0 ± 2.6*	212 ±	116.8*	7.1 ± 4.10*
17	41.7 ± 4.9	1127 ±	1038.8	26.3 ± 22.98
19	41.3 ± 4.9	1720 ±	993.8	42.2 ± 23.48
21	44.0 ± 6.0*	3137 ±	203.1*	71.8 ± 5.70*

* Statistically significant, $P<0.05$.

observed to be exponential.

Formation of Pericardial Pores

The pericardia we observed in newborn mice consisted of two mesothelia, pericardial and pleural, that sandwiched a thin connective tissue layer (Fig. 3). This trilaminar structure did not differ from that of the pericardia in adult mice (Nakatani *et al.*, 1988). Most intercellular abutments in the mesothelia were tight junctions (Fig. 3, inset), although some desmosome-like junctions were also observed. The basal lamina underneath the mesothelia was discontinuous. Occasionally, short cytoplasmic processes extended from pericardial mesothelial cells into sparse connective tissue and approached the basal surface of the pleural mesothelium (Fig. 4). Conversely, cytoplasmic processes of pleural mesothelial cells approached the base of the pericardial mesothelium. Connective tissue elements were often absent or extremely sparse near these cytoplasmic processes. Also, the basal lamina was often lacking; thus, the cell membranes of the mesothelia were closely associated and adjoined principally with tight junctions. This vertical connection between the pericardial and pleural mesothelia resulted in the formation of a pair of U-shaped folds with one limb of each U formed by pericardial mesothelial cells and the other by pleural mesothelial cells, each surrounding bundles of connective tissue (Fig. 5). In figures 5 and 6 pairs of U-shaped folds were connected at their apices with tight junctions, thus creating a horizontal connection that preserved the continuity of the pericardium. In TEM, pericardial pores appeared as spaces between pairs of U-shaped folds (Fig. 7). We propose that the

pores are formed when horizontal connections, like those in figures 5 and 6, separate, although we are unsure of the mechanism.

Scanning electron microscopy was employed to count the number of pores, however, it was additionally used for observation of surface changes of the pericardium. There were many pores which were divided into small compartments by thready extensions of mesothelial cells (Figs. 8 and 9). Granular cytoplasmic extrusions were also found in the marginal zone of pericardial pores (Fig. 9). In an area of the lacy appearance adjacent pores were often separated by a thin strap of mesothelium (Fig. 10).

Discussion

In this study we assert that the pericardial pores are absent until P6 and first appear on P7. The number of pericardial pores per pericardium is approximately 2 on P7 and increases with age to reach 3000 on P21. The number of pericardial pores per pericardium is assumed to increase further, since our previous study (Nakatani *et al.*, 1988) showed that the number became fairly stable between postnatal weeks 6 and 11, reaching as many as 64,000.

We think that the pericardial pores are formed in three stages: (1) a stage of vertical connection during which the pericardial and pleural mesothelia are attached to one another to form U-shaped folds, (2) a stage of horizontal connection during which a pair of U-shaped folds are interconnected at their apices with tight junctions, and (3) a stage of separation of the pair of U-shaped folds. The first and second stages may proceed concomitantly.

It is known that the basal lamina of the peritoneal mesothelium (Carr, 1967; Leak and Rahil, 1978) and ovarian bursa (Nakatani *et al.*, 1986) is often lacking or discontinuous. This is also true of the mouse pericardium. Especially where events in the first and second stages occurred, the basal lamina was consistently absent and connective tissue elements were extremely sparse. This seems to be relevant since cell-to-cell contact with tight junctions is only possible where there is no intervening structure between the cells. Interesting is a similarity of these events with events that occur prior to rupture of the buccopharyngeal membrane. According to Waterman (1977) and his associates (Waterman and Schoenwolf, 1980) the stomodeal ectoderm and foregut endoderm of the hamster embryo become closely apposed by extension of cytoplasmic processes to the opposing germ layer. Intermingling of cells subsequently occurs within the membrane, and some cells extend the entire width of the membrane with surfaces exposed to both foregut and stomodeum. During these events an originally distinct basal lamina

is phagocytosed by the epithelium and becomes discontinuous to allow extension of the cytoplasmic processes. The only difference is that the pericardial mesothelium did not show phagocytotic activity, but we do not think that the activity is necessary since the golden hamster pericardium originally lacks continuous basal lamina.

We assume that the pericardial pores are formed by separation of tight junctions between the U-shaped folds, but what triggers the separation remains uncertain. Tight junctions are not necessarily stable structures, as has been thought, but are separable under various experimental conditions (Goodenough and Gilula, 1974; Meldolesi *et al.*, 1978; Porvanznik, 1979). According to Decker and his associates (1974 and 1981) disassembly of tight junctions occurs during amphibian neurulation; i.e. tight junctions become attenuated initially, fragment into domains composed of fibrillar remnants and particulate arrays in P-face profile and finally vanish. Important is an observation that the disassembly of tight junctions occurs concomitantly with peripheral cytoskeletal activity remodeling cell borders (Pitelka *et al.*, 1983). The pericardial and pleural mesothelia during the period of our observations might have been very dynamic. It is possible that they multiplied, widened and changed their cell shape, since the pericardium on P21 was three times wider than on P1. This means that the cytoskeleton of the mesothelial cells underwent remarkable changes, and tight junctions connecting U-shaped folds might have disappeared.

Some authors think that tension produced by differentials in rates of cell proliferation triggers rupture of the buccopharyngeal membrane (Miller and Olcott, 1989). Similarly, mechanical reasons should be considered to account for perforation of the pericardium. The pericardium is incessantly exposed to the dynamic movements of the heart and lungs, and focal tension is assumed to be produced on the pericardium. In addition to disappearance of tight junctions, focal tension may work to enhance the separation of U-shaped folds. Watanabe *et al.* (1984) suggested that focal degeneration of cells lining the buccopharyngeal membrane may exert for rupture of the membrane. We still did not find clear morphological evidence for mesothelial cell degeneration, but an involvement of cell degeneration in perforation of the pericardium may not be altogether negative.

Acknowledgement

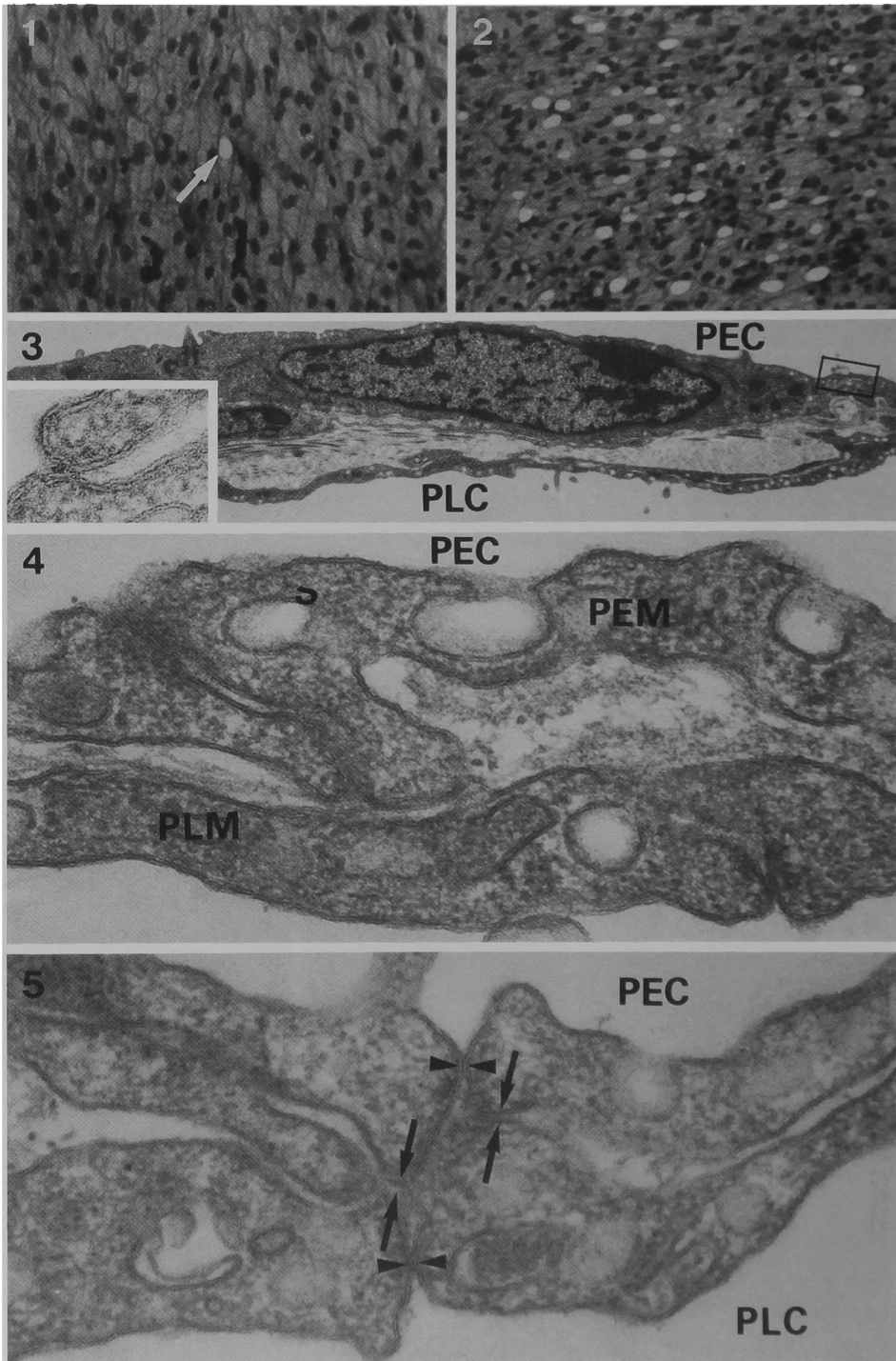
The authors thank Mr. T. Horii, and Miss H. Matsuda for technical assistance, and Mrs. H. Nakatani and F. Fukuo for typing the manuscript. We are grateful to Mr. Ryan P. McGuinness of the University of California at Davis for his critical revision.

Literature Cited

- 1) Carr, I.: The fine structure of the cells of the mouse peritoneum. *Z. Zellforsch.*, **80**: 534-555, 1967.
- 2) Decker, R.S. and D.S. Friend: Assembly of gap junctions during amphibian neurulation. *J. Cell Biol.*, **62**: 32-47, 1974.
- 3) Decker, R.S.: Disassembly of the zonula occludens during amphibian neurulation. *Dev. Biol.*, **81**: 11-22, 1981.
- 4) Fukuo, Y., T. Nakatani, H. Shinohara and T. Matsuda: The mouse pericardium: It allows passage of particulate matter from the pleural to the peritoneal cavity. *Anat. Rec.*, **222**: 1-5, 1988.
- 5) Goodenough, D.A. and N.B. Gilula: The splitting of hepatocyte gap junctions and zonulae occludentes with hypertonic disaccharides. *J. Cell Biol.*, **61**: 575-590, 1974.
- 6) Leak, L.V. and K. Rahil: Permeability of the diaphragmatic mesothelium: the ultrastructure basis for "stomata". *Am. J. Anat.*, **151**: 557-594, 1978.
- 7) Meldolesi, J., G. Castiglioni, R. Parma, N. Nassivera and P. DeCamilli: Ca-dependent disassembly and reassembly of occluding junctions in guinea pig pancreatic acinar cells. Effect of drugs. *J. Cell Biol.*, **79**: 156-172, 1978.
- 8) Miller, S.A. and C.W. Olcott: Cell proliferation in chick oral membrane lags behind that of adjacent epithelia at the time of rupture. *Anat. Rec.*, **223**: 204-208, 1989.
- 9) Mironov, V.A., S.A. Gusev and A.F. Baradi: Mesothelial stomata overlying omental milky spots: scanning electron microscopic study. *Cell Tissue Res.*, **201**: 327-330, 1979.
- 10) Mixer, R.L.: On macrophagal foci ("milky spots") in the pleura of different mammals, including man. *Am. J. Anat.*, **69**: 159-186, 1941.
- 11) Nakatani, T., H. Shinohara and T. Matsuda: On the ovarian bursa of the golden hamster. II. intercellular connections in the bursal epithelium and passage of ferritin from the cavity into lymphatics. *J. Anat.*, **148**: 1-12, 1986.
- 12) Nakatani, T.H., H. Shinohara, Y. Fukuo, S. Morisawa and T. Matsuda: Pericardium of rodents: pores connect the pericardial and pleural cavities. *Anat. Rec.*, **220**: 132-137, 1988.
- 13) Pitelka, D.R., B.N. Taggart and S.T. Hamamoto: Effects of extracellular calcium depletion on membrane topography and occluding junctions of mammary epithelial cells in culture. *J. Cell Biol.*, **96**: 613-624, 1983.
- 14) Porvaznik, M.: Tight junction disruption and recovery after sublethal irradiation. *Radiat. Res.*, **78**: 233-250, 1979.
- 15) Snell, G.D.: Reproduction. In: *Biology of the laboratory mouse*. G.D. Snell, ed. Dover Publications, Inc. New York, pp. 55-88, 1961.
- 16) Watanabe, K., F. Sasaki and H. Takahama: The ultrastructure of oral (buccopharyngeal) membrane formation and rupture in the anuran embryo. *Anat. Rec.*, **210**: 513-524, 1984.
- 17) Waterman, R.E.: Ultrastructure of oral (buccopharyngeal) membrane formation and rupture in the hamster embryo. *Develop. Biol.*, **58**: 219-229, 1977.
- 18) Waterman, R.E. and G.C. Schoenwolf: The ultrastructure of oral (buccopharyngeal) membrane formation and rupture in the chick embryo. *Anat. Rec.*, **197**: 441-470, 1980.

Explanation of Figures**Plate I**

- Figs. 1 and 2. Spread specimens of the pericardium stained with toluidine blue. The solitary pericardial pore indicated by the arrow was found in the pericardium on P7 (Fig. 1). Note the lacy appearance of the pericardium on P17 (Fig. 2). Fig. 1; $\times 125$, Fig. 2; $\times 125$.
- Fig. 3. The pericardium consists of the pericardial and pleural mesothelia sandwiching connective tissue in between. The mesothelial cell has a spindle-shaped or oval nucleus, attenuated cytoplasm, numerous caveolae and microvilli. Adjacent cells are connected with tight junctions (inset). The basal lamina is discontinuous in some places. Square indicates inset. PEC: pericardial cavity, PLC: pleural cavity. $\times 8500$, Inset; $\times 12000$.
- Fig. 4. The cytoplasmic processes of the pericardial mesothelium approach the base of the pleural mesothelium. Note the absence of basal lamina and sparse connective tissue. PEM: pericardial mesothelial cell, PLM: pleural mesothelial cell. $\times 140000$.
- Figs. 5 and 6. The pericardial and pleural mesothelia are connected to one another (arrows) forming U-shaped folds. A pair of U-shaped folds are adjoined with tight junctions at their apices (arrowheads). Fig. 5; $\times 146000$, Fig. 6; $\times 46000$.



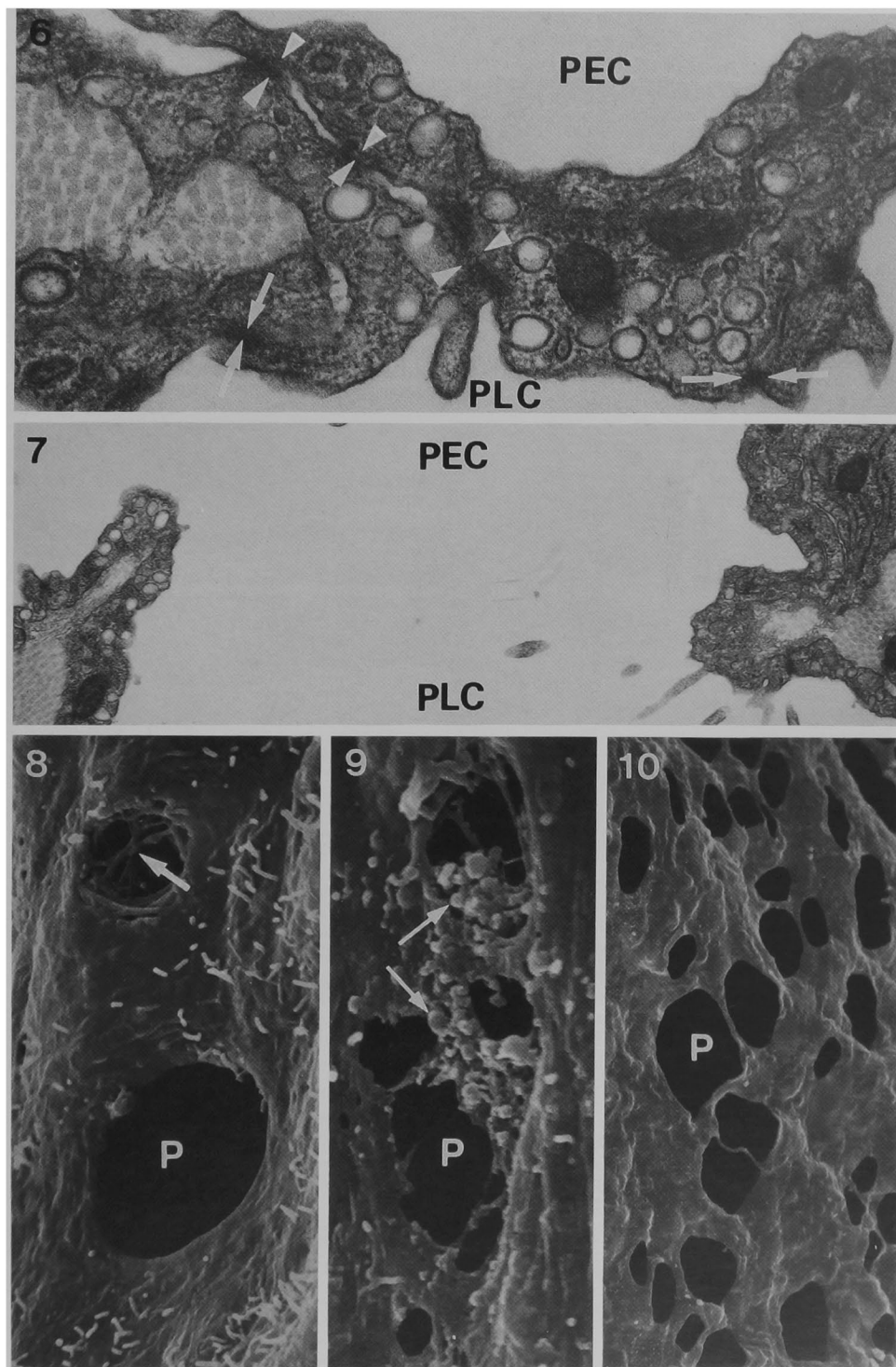


Plate II

- Fig. 7. The pericardial pore is a channel formed between U-shaped folds and connects the pericardial and pleural cavities. The pore may emerge when the tight junctions connecting a pair of U-shaped folds (Figs. 5 and 6) separate and/or disappear. $\times 22000$.
- Fig. 8. Pericardial pores on P9. The arrow indicates cytoplasmic processes dividing a pore. P: pericardial pore. $\times 3700$.
- Fig. 9. Pericardial pores on P15. Vesicular cytoplasmic extrusions (arrows) are often located in the marginal zone of pericardial pores. $\times 60000$.
- Fig. 10. An area of the lacy appearance on P21. Note that adjacent pores are divided by a thin strap of the mesothelium. $\times 500$.